Regular Article

PHYSICAL CHEMISTRY RESEARCH
Published by the
Iranian Chemical Society
www.physchemres.org
info@physchemres.org

***Phys. Chem. Res.**, Vol. 4, No. 2, 231-243, June 2016*
DOI: 10.22036/pcr.2016.13940

Halogenated Graphdiyne and Graphyne Single Layers: A Systematic Study

F. Houshmand[a], S. Jalili[a,b,*] and J. Schofield[c]

[a]*Department of Chemistry, K. N. Toosi University of Technology, P.O. Box: 15875-4416, Tehran, Iran*

[b]*Computational Physical Sciences Research Laboratory, School of Nano-Science, Institute for Research in Fundamental Sciences (IPM), P.O. Box: 19395-5531 Tehran, Iran*

[c]*Chemical Physics Theory Group, Department of Chemistry, University of Toronto, 80 Saint George Street, Toronto, Ontario, Canada M5S 3H6*

(Received 23 January 2016, Accepted 25 March 2016)

Graphyne and graphdiyne families of flat carbon (sp^2/sp) networks with high degrees of π-conjunction are attracting much attention due to their promising electronic, optical, and mechanical properties. In the present investigation we have studied the structural, mechanical, electrical and optical properties of halogenated graphdiyne and graphyne. The optical spectra of pure and halogenated structures are calculated. The optical absorption is dominated by excitonic effects with a high electron-hole binding energy within the Bethe-Salpeter equation. Band structures of graphdiyne and halogenated graphdiyne show that these nanostructures are semiconductors with a direct band gap of ~0.5 eV at the center of Brillouin zone. Halogenation of graphdiyne can effectively modulate the band gap. The second-order elastic constants and other related quantities such as the Young's modulus and Poisson's ratio have also been calculated in the present work.

Keywords: Graphdiyne, Halogenated graphdiyne, Bethe-Salpeter equation, Many-body perturbation theory, Optical spectra, Density functional theory

INTRODUCTION

The adsorption of halogen gases on graphene has several applications in different fields, from promoting neuro-induction of stem cells to the fabrication of micro-batteries with superlative efficiency. Researchers even search for more ideal materials to be superseded with graphene, aiming to better efficiency and less undesirable features such as hydrophobicity [1-4]. A new family of carbon nano-materials known as super-graphene structures are attracting many researchers. One example is single-layer Graphdiyne (pGD) with hexagonal carbon rings and carbon-carbon triple-bond linkages [5]. It has been recognized as a superior candidate material to use in the next generation of semiconductor devices and to break the classical limitation of silicon-based opto-electronic devices [6]. The large-area nano-films with an acceptable quality of graphdiyne have been fabricated very recently [7]. This highly conductive structure also exhibits remarkable chemical stability. Recently, we have reported the high field-effect carrier mobility of pGD sheets and nanotubes. We have shown that the same level of charge carrier mobility as graphene exists in this family [8].

Recent studies by Luo *et al*. indicated that graphdiyne exhibits interesting excitons with both Wannier-Mott and Frenkel characteristics [9-10]. They also demonstrated that the theoretical prediction of low-energy optical absorption spectra of multi-layer graphdiyne strongly depends on the van der Waals correlation. Due to a large excitonic binding energy (over 0.55 eV) and large mechanical stability, single-layer graphdiyne is predicted to be an excellent material for optoelectronic devices.

A variety of halogenated conjugated systems are used in electronic devices such as electroluminescent diodes or

*Corresponding author. E-mail: sjalili@kntu.ac.ir

field-effect transistors [11-13]. In particular, halogen atoms lower both the HOMO and LUMO energy levels and as a consequence, the electron injection is made easier, which can often result in ambipolar semiconductors. Fluorination of carbon nano-materials has many advantages due to the unique nature of the carbon-fluorine (C-F) bond. For instance, the C-F bond demonstrates excellent oxidative and thermal stability, high polarity and low surface free energy. Moreover, C-X bonds play an important role in the solid state supramolecular organization, originating a typical pi-stack arrangement which enhances the charge carrier mobility [14]. Such interesting characteristics have encouraged researchers to investigate the fluorinated graphene over the past few years.

Herein we investigate the photo-spectra of halogenated structures at different concentrations of adsorbed halogen atoms in order to find the influence of many-body effects on the electronic structure and optical absorption of halogenated graphdiyne (pGD) or graphyne (pGY) which are entirely dominated by the interacting photo-excited electron-hole pairs. After a systematic study of opto-electronic properties of pGD and pGY, we will compare the properties of pGD/pGY with those of halogenated pGD/ pGY.

COMPUTATIONAL DETAILS

The ground-state calculations were performed for isolated systems by using density functional theory (DFT) approach, as implemented in the Quantum ESPRESSO package [15]. A plane-wave basis set was used with a cut-off of 50 Ry and norm-conserving pseudopotentials [16]. To improve the band structures obtained at the DFT level and to simulate the optical spectra, electron-electron and electron-hole corrections were calculated within the framework of many-body perturbation theory. Quasi-particle corrections to the Kohn-Sham eigenvalues were calculated within the G_0W_0 approximation for the self-energy operator, where the dynamic dielectric function was obtained within the plasmon-pole approximation. The Coulomb potential was truncated by using a box-shaped cutoff to remove the long-range interactions between periodic images. The optical absorption spectra were then computed as the imaginary part of the macroscopic dielectric function starting from the solution of the Bethe-Salpeter equation (BSE). The static screening in the direct term was calculated using the random-phase approximation by including the local field effects. The Tamm-Dancoff approximation for the BSE Hamiltonian was employed. The aforementioned many-body effects were included using the YAMBO code [17]. The ground-state structural calculations such as mechanical properties and optical spectra were performed by SIESTA package [18], utilizing a double-zeta polarized (DZP) basis set. After the evaluation of the active bonding sites for X (= F, Cl) atoms and the probable recombination paths, the activation energy along that path was calculated to predict the kinetics of the recombination reaction. An initial path was constructed and represented by a discrete set of images of the system connecting the initial and final states. To calculate the activation energy barrier, the nudged elastic band (NEB) [19] method implemented in the Quantum ESPRESSO package was used.

RESULTS AND DISCUSSION

Structural Properties

There are many experimental evidences for aggregation of halogen atoms with each other on graphene and thereby it seems that the synthesis of halogenated graphene for a variety of potential applications is faced with an obstacle. Recent investigations and experimental effort [7] showed the possibility of successful synthesis of graphdiyne films and flakes. So, this porous structure with large surface area can be used in many applications such as in future opto-electronic devices [20]. It was demonstrated theoretically that the single layer of graphyne can preferentially adsorb halogen atoms and form sp^2-hybridized bonds [21]. The structural parameters of halogenated pGD/pGY obtained by DFT method are listed in Table 1. We typically set the structural optimization method to allow variable cell relaxation for fully halogenated graphdiyne and graphyne. The halogenated systems maintain a perfect hexagonal symmetry, similar to that observed for pristine graphdiyne and graphyne. The unit cell of fluorinated pGD is slightly expanded with respect to the graphdiyne's, in contrast to the case of hydrogenated graphdiyne which shows a compressed lattice. We studied fully halogenated graphdiyne and graphyne (n = 1) and also partially

Table 1. Structural Properties of Halogenated Graphdiyne and Graphyne: Structural Parameters: Halogen-carbon-carbon Angle, Halogen-Carbon Bond Length, d_1 ($C_{sp} \equiv C_{sp}$) bond length, d_2 ($\equiv C_{sp}$ - $C_{sp} \equiv$) and Cohesive Energy, Activation Energy

	α (*X* - *C* - *C*)	d_{C-X}	d_1	d_2	E_{coh} (eV/atom)	E_α (eV)
F_2-Graphene	89	1.37[a]	1.45	-	25.31[a]	1.5[b]
Cl_2-Graphene	87	1.73[a]	1.45	-	19.60[*]	-
F_2-pGD	87	1.42	1.44	1.37	7.24	1.12
Cl_2-pGD	88	1.74	1.45	1.39	5.12	1.85
F_2-pGY	83	1.37	1.50	-	6.98	1.91
Cl_2-pGY	85	1.72	1.51	-	3.29	2.36

[a]For 5*5 super cell of fully halogenated graphene[18]. [b][19].

halogenated single layers (n = 0.75, 0.5); where n demonstrates carbon to halogen concentration ratio.

To evaluate the stability of the systems, cohesive energy was calculated from $E_{coh} = E_{tot} - nE_C$, where E_{tot} denotes the spin-polarized total energy of fully optimized planar graphdiyne and graphyne and n and E_C are the number of carbon atoms and the total energy of a single carbon atom, respectively. Both energy terms were evaluated using a same supercell size. Table 1 shows the results for pGD and pGY as well as the halogenated pGD. The calculated cohesive energy for halogenated pGD indicates that their stability is in a same range as pGD.

In the case of single fluorine and chlorine molecule, the halogen atoms adsorb on *sp*-bonded atoms in graphdiyne and graphyne. However, there are three other sites on hexagonal rings with sp^2-bonded carbon atoms. Nudged elastic band (NEB) calculation (Table 1) for the adsorption of halogen molecules on pGD (pGY) shows that, by increasing the concentration of halogen atoms, the sp^2 carbons in the rings become suitable for adsorption (Fig. 1). In fact, the powerful tendency of halogen atoms to aggregate avoids the stability of halogenated graphdiyne and graphyne with saturated *sp-sp* bonds. In addition, it seems that holding the symmetry and integration is also an important factor to stabilize the halogenated pGD (pGY) with a same number of carbon and halogens atoms. According to the results in Table 1 and Fig. 1, the most stable structure for halogenated graphdiyne is the nano sheet with the same number of halogen atoms above and below the single layer of graphdiyne (graphyne). Figure 1 shows that the excitation states in case of pGD-F_2 with n = 1 are in less energy level compared to other possible structures studied here. Results of activation energy for halogenation reaction (Table 1) also show that the halogenation of pGD is a more suitable process compared to halogenation of graphene and graphdyne. On the other hand, adsorption of chlorine atoms on both pGD and pGY yields more bended carbon-carbon bond compared to fluorine. Therefore, chlorinated pGD (pGY) are less stable than fluorinated structures. However, chlorinated graphdiyne (n = 1) is more stable than graphyne case.

Elastic Constants and Mechanical Stability

The elastic constants of solids provide a link between the mechanical and dynamical behavior of crystals and give important information concerning the nature of the forces operating in solids. In particular, they provide information on the stability and stiffness of materials, but their *ab initio* calculation requires precise methods. Since the forces and the elastic constants are functions of the first order and second order derivatives of the potentials, their calculation will provide a further check on the accuracy of the

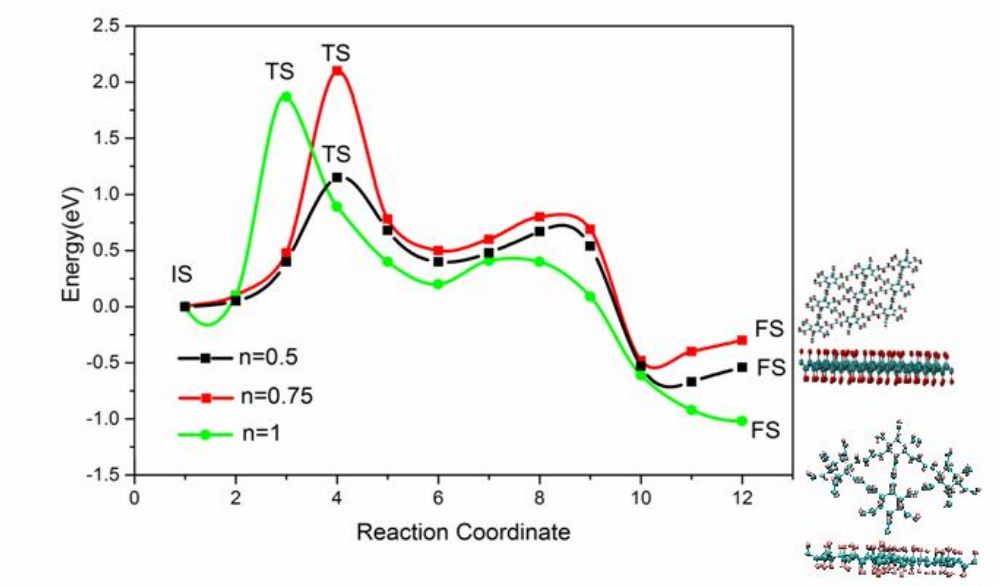

Fig. 1. FT-IR spectra of $ZnFe_2O_4$@SiO_2-NH_2-TCT (a) without and (b) with immobilization of beta-amylase enzyme.

calculation of forces in solids. They also provide valuable data for developing inter-atomic potentials [23]. To compute the elastic constants we have used the "volume-conserving" technique [24] in SIESTA. Young's modulus is defined as the ratio of stress to strain, and is used to provide a measure of the stiffness of the solid. The material is stiffer if the value of Young's modulus is high. The value of the Poisson's ratio indicates the degree of directionality of the covalent bonds. The value of the Poisson's ratio is small (υ = 0.1) for covalent materials, whereas for ionic materials a typical value of υ is 0.25 [25].

In order to study the mechanical properties of bulk halogenated pGY and pGD, the elastic constants C_{ij}, bulk modulus B, shear modulus G, Young's modulus Y, and Poisson's ratio υ when maximum deformation magnitude (η_{max}) is set to 1×10^{-2} were calculated. In this calculation the intermediate deformation between η_{-max} and η_{max} is 10. The calculated results are shown in Table 2. According to Ref. [23], both Laue classes of the hexagonal crystal system have five independent elastic constants. These elastic constants are (C_{11}, C_{12}, C_{13}, C_{33}, C_{44}) and the sixth constant is C_{66} = (C_{11} - C_{12})/2. By direct calculation of the eigenvalues of the stiffness matrix, one can derive the following four necessary and sufficient conditions for elastic stability in the hexagonal case (Born stability criteria):

$$\{C_{11} > |C_{12}|; 2C_{13}^2 < C_{33}(C_{11} + C_{12}) \quad C_{44} > 0; C_{66} > 0 \tag{1}$$

It is shown that the Born stability criteria are satisfied for both chlorinated and fluorinated pGD and hence they are mechanically stable under elastic strain perturbations. The values of C_{11} for both chlorinated and fluorinated pGD are smaller than those of pristine graphdiyne, which show relatively lower resistances against the principal strain ε_{11}. The C_{44}-value of fluorinated pGD (40 GPa) is larger than that of graphdiyne indicating higher resistance to basal and prismatic shear deformations compared to graphdiyne.

It is useful to estimate the corresponding parameters for the polycrystalline and nano-materials. The theoretical polycrystalline and nano-structures' elastic moduli for all structures studied here may be calculated from the set of six elastic constants. Hill [26-27] proved that the Voigt and Reuss equations represent upper and lower limits of the true polycrystalline constants. Hill showed that the polycrystalline moduli are the arithmetic mean values of the moduli in the Voigt (BV, GV) and Reuss (BR, GR)

Table 2. Mechanical Properties of Halogenated Graphdiyne and Graphyne: Poisson Ratio, In-plane and out of Plane Young Modulus, Ratio of Shear Modulus/Bulk Modulus, Anisotropic Factor at Zero Pressure (all in GPa)

	n	Poisson ratio			Young's modulus		G/B			A
		XX	XY	YZ	E_A^{2D}	E_B^{2D}	Reuss	Voigt	Hill	
pGD	-	0.4012	0.5610	1.1798	18.4754	18.2451	0.1150	0.2540	0.3010	0.84
	1.00	0.4224	0.7819	1.2135	45.8764	41.4843	0.2210	0.3990	0.3110	0.32
pGD-F	0.50	0.3265	0.0116	0.0161	32.1235	30.2889	0.4080	0.4340	0.4330	0.46
	0.75	1.2239	0.3788	0.2013	-77.3879	-724.8882	0.4610	-0.5330	0.7160	0.53
	1.00	0.4307	0.0071	0.0081	36.5225	36.3719	0.3810	0.5070	0.5500	0.15
pGD-Cl	0.50	0.8664	0.2602	0.3397	43.5362	35.2598	0.2400	-0.0770	0.0400	0.08
	0.75	0.0061	0.5619	8.6530	-29.1041	-0.0217	-0.2950	0.4110	0.4710	0.03
pGY	-	0.2219	0.1147	0.1953	16.2145	16.3293	0.0210	0.3512	0.3321	0.75
	1.00	0.4134	0.1099	0.1691	33.6577	54.3520	0.6770	0.4270	0.5680	0.89
pGY-F	0.50	0.6213	0.0115	0.0121	51.3215	56.9546	0.3210	0.5412	0.2139	0.09
	0.75	0.0031	0.0294	0.3641	-30.1154	-13.2541	-0.3691	0.5142	0.6210	0.05
	1.00	0.2926	0.0207	0.5375	34.8009	33.8117	0.3950	0.7730	0.5600	0.79
pGY-Cl	0.50	0.5795	0.1654	0.2298	41.9345	40.9876	0.4130	-0.8450	0.0980	0.07
	0.75	0.0078	0.4321	0.9871	-30.8421	-21.0215	-0.3540	0.3590	0.5190	0.01

approximation, and are thus given by Hill's bulk modulus, BH ≡ B = ½(BR + BV), where BR and BV are the Reuss's and Voigt's bulk modulus respectively. Hill's shear modulus is GH ≡ G = ½(GR + GV), where GR and GV are the Reuss's and Voigt's shear modulus, respectively. The expression for Reuss and Voigt moduli can be found in Ref. [27]. The polycrystalline Young's modulus *Y*, and Poisson's ratio v, are then computed from these values using the relationships: $Y = 9BG/(3B + G)$, $v = (3B - Y)/6B$. We note that the Young's modulus *Y* of pGD-F is larger than that of pGD-Cl. Therefore, the pGD-F compared to pGD-Cl shows a better performance of the resistance to shape change and against uniaxial tensions. We also note that the bulk modulus *B* of pGD-F is higher than that of pGD-Cl.

The so called shear anisotropy factor, $A = 2C_{44}/(C_{11} - C_{12})$ is often used to represent the elastic anisotropy of crystals [26]. A value of $A = 1$ represents completely elastic isotropy, while values smaller or greater than this measure the degree of elastic anisotropy. It is clear from Table 2 that both pGD-F and pGD-Cl show completely anisotropic behaviour.

One of the most widely used malleability indicators of materials is Pugh's ductility index (*S*/*B*) [28]. As is known, if the ratio of *S*/*B* is less than 0.5 the material will have a ductile behaviour, whereas if *S*/*B* > 0.5 the material is brittle. According to this indicator (Table 2), both halogenated graphdiyne and graphyne are near the borderline of brittleness. The partially halogenated

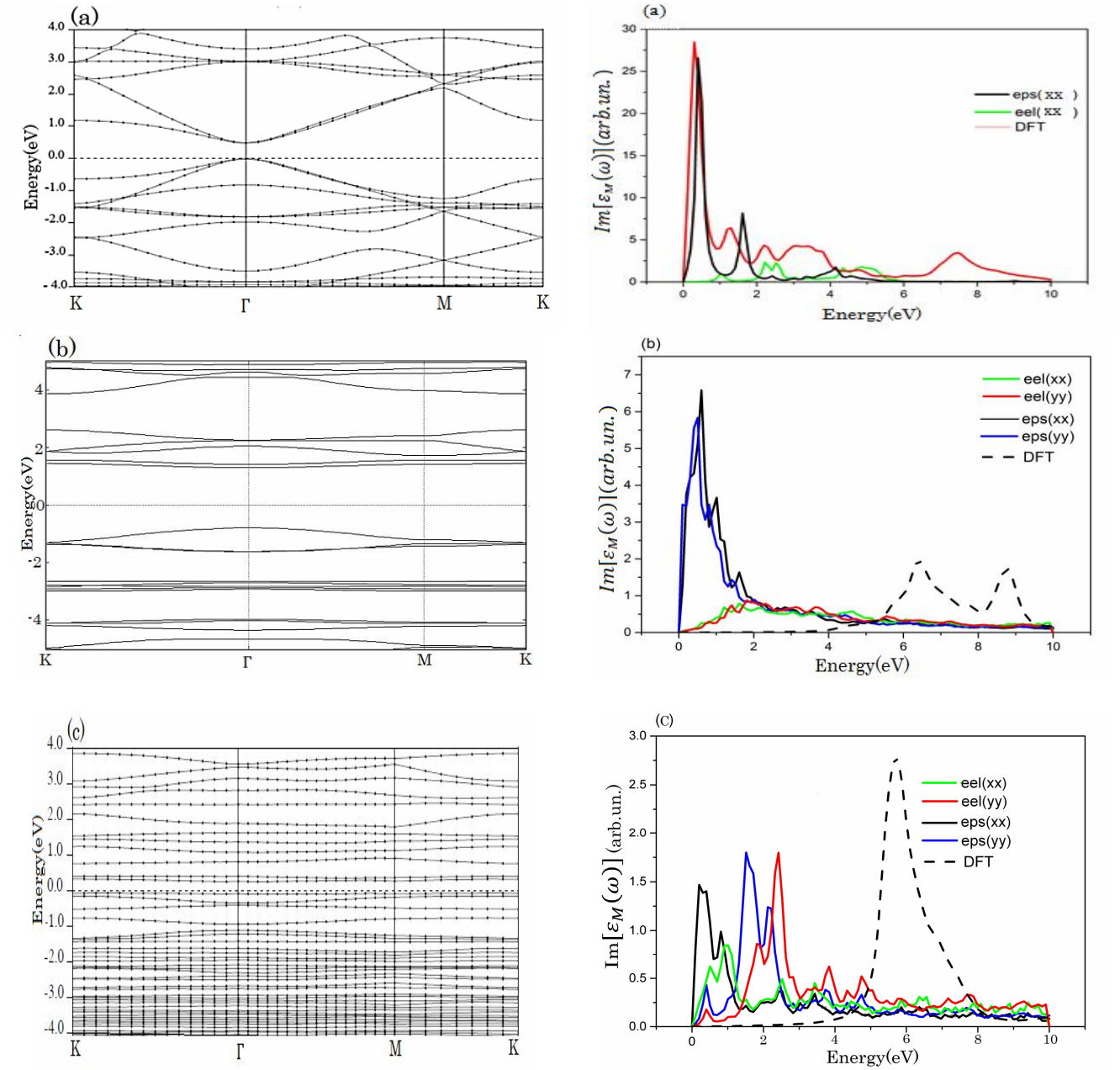

Fig. 2. Band structures (left) and calculated absorption spectra (right) along *x* and *y*-directions for (a) pGD (b) pGD-F (n = 0.5) (c) pGD-F (n = 1) (d) pGD-Cl (n = 0.5) (e) pGD-Cl (n = 1).

graphdiyne and graphdyne with n = 0.75 display the negative magnitudes. The negative magnitude of bulk modulus is usually due to uniquely oriented, hinged molecular bonds.

Finally, the obtained values of the Poisson's ratio from DFT method for bulk configuration of studied structures are listed in Table 2. As is known, the Poisson's ratio for brittle covalent materials has a small magnitude whereas for

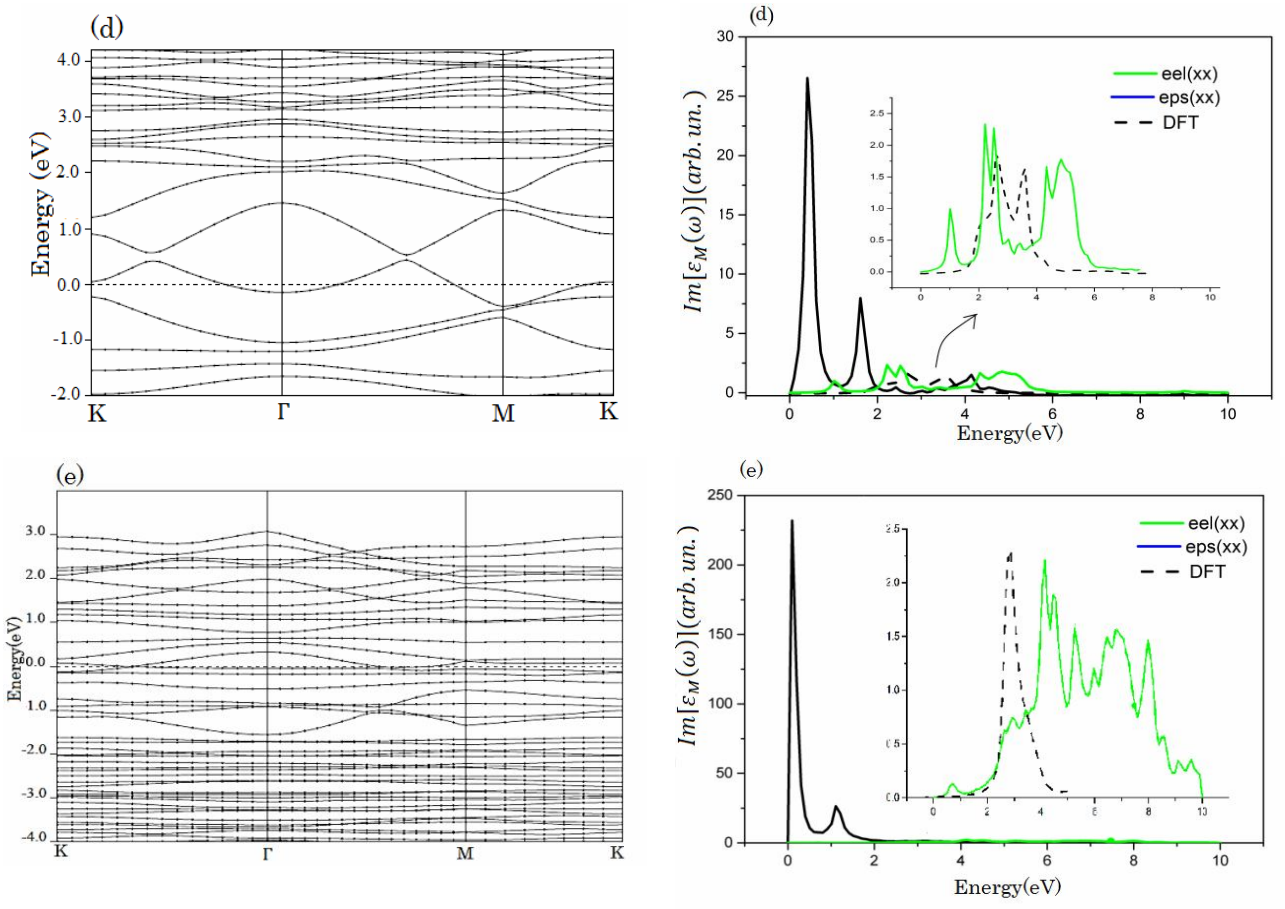

Fig. 2. Continued.

metallic materials it is around 0.33 [29]. Thus, halogenated pGD and also pGY (in n = 1, 0.5) show the characteristics of being more in the latter category.

Electrical and Optical Properties

In this section we investigate the band gap and optical properties of graphdiyne (pGD) and graphyne (pGY) after halogenation. Band structure of pGD (Fig. 2a, left) indicates that this nanostructure is a direct band gap semiconductor with the minimum band gap in the centre of Brillouin zone (~0.5 eV). Recent *ab initio* studies have shown that excitonic effects dramatically alter the optical response of low dimensional structures. So, herein we carried out a first principle calculation, including the relevant many-electron (quaosiparticle self-energy and electron-hole interaction) effects to study the optical properties of single layer graphdiyne and graphyne. This carbon material is expected to show impressive properties for optical application. Fig. 2a, shows the optical diagram of pGD computed from the solution of the BSE. The imaginary part of the macroscopic dielectric function shows that pGD exhibits excitons with both Wannier-Mott and Frenkel characteristics which confirm the experimental results [9-10]. Adsorption of halogen atoms on pGD has an impressive effect on the electronic structure. Figure 1 illustrates the band structure of pGD(pGY), Chlorinated Graphdiyne (graphyne) and Fluorinated Graphdiyne (graphyne). As Figs. 2 and 3 show, adsorption of halogen on pGD directly affects the magnitude of bandgap. However, in contrast to halogenated graphene which is insulator, the halogenated pGD (pGY) is still semiconductor with a different band gap.

The in-plane and out of plane imaginary electron-electron part of dielectric function (G-space) in case of pGD is coincident but this coincidence is missing in pGY case.

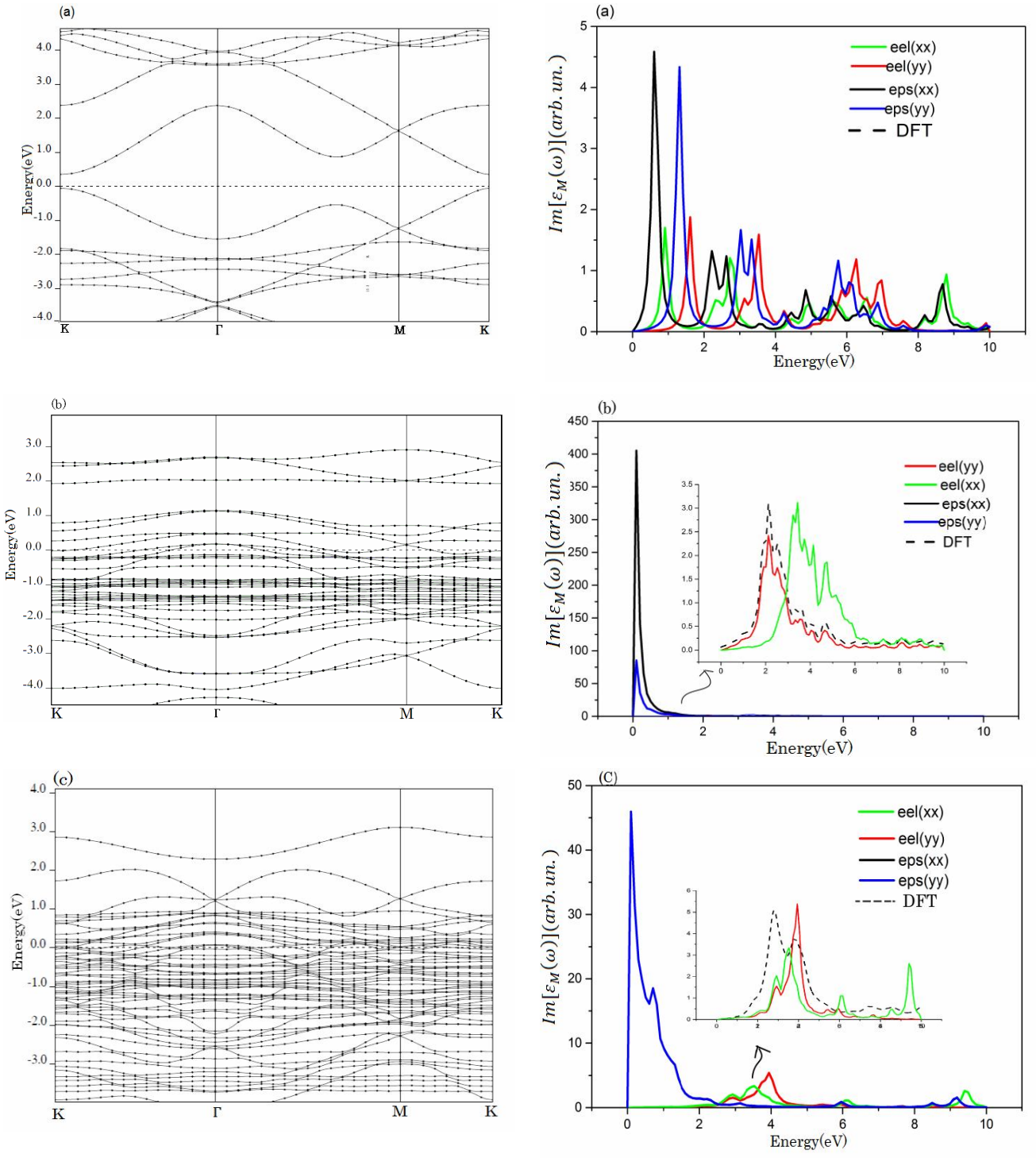

Fig. 3. Band structures (left) and calculated absorption spectra (right) along *x* and *y*-directions for (a) pGY (b) pGY-F (*n* = 0.5) (c) pGY-F (*n* = 1) (d) pGY-Cl (*n* = 0.5) (e) pGY-Cl (*n* = 1).

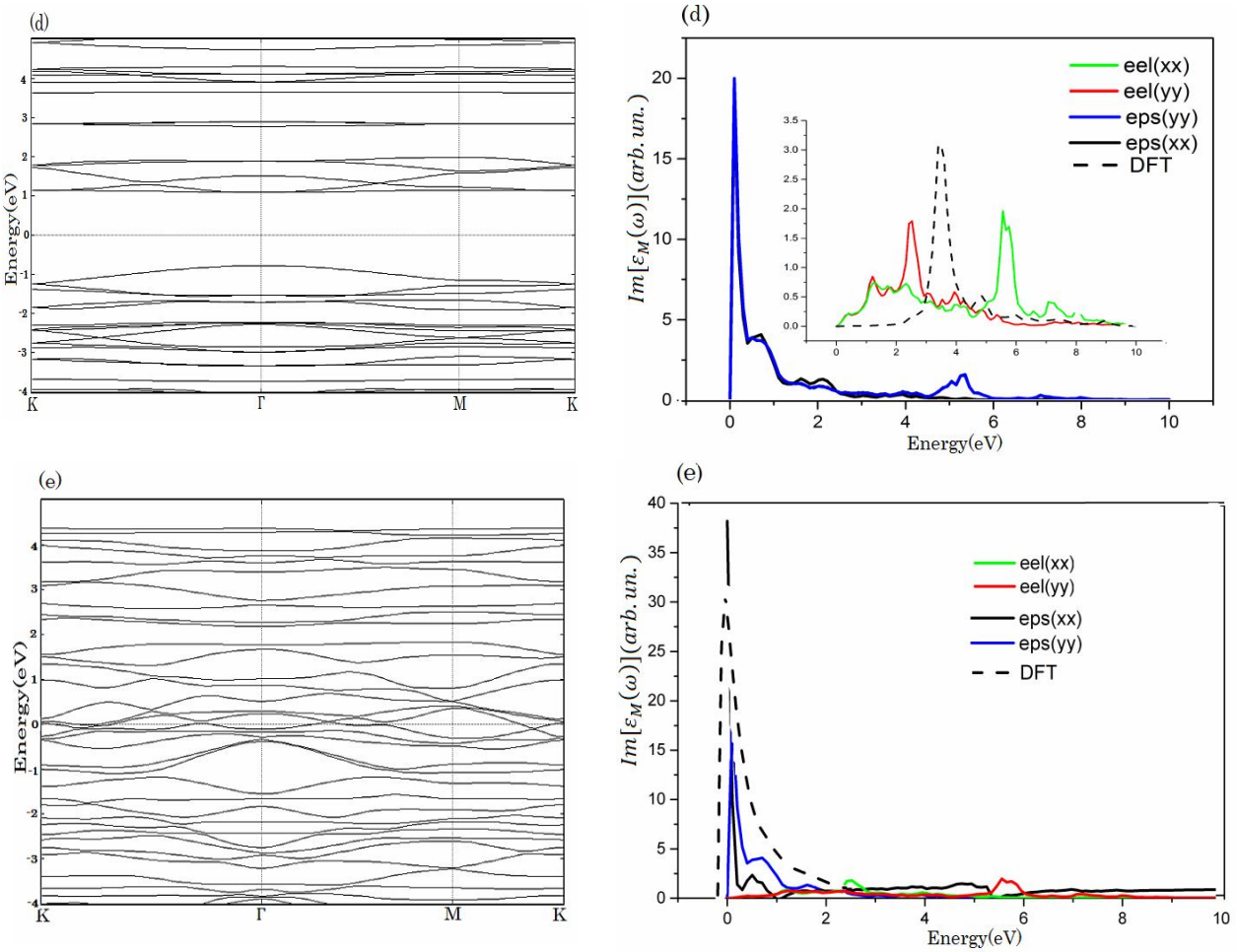

Fig. 3. Continued.

The in-plane and out of plane imaginary electron-phonon part of dielectric function (eh-space) has the same behaviour. By adsorption of halogen atoms this feature misses and two components are distinct. The imaginary part of dielectric function obtained from density functional theory in all cases is substantially disjoint from one obtained from BSE method (Figs. 2 and 3). This feature confirms the effective influence of exciton interaction in optical absorption in these 2D materials. In addition, fluorinated pGD with n = 1 (Fig. 2c) shows obviously different optical absorption peaks with others (Fig. 2) and this difference is also seen in band structures. DFT method shows the absorption peak in totally incorrect energy and this feature indicates the importance of exciton effect in this case. Separation of in-plane components (*xx* and *yy* directions) can be effectively used in chemical study of these structures. In contrast to fluorine, chlorine atom causes a different effect on band structure and optical spectrum of graphdiyne. In this case, band structure shows effective divergence in energy gap and energy gap of transfers to different points of Berillouin zone. The major effect of this integration in energy gap is decreasing the absorption region in low energies. In fact, absorption spectrum shows a single peak in chlorinated graphdiyne (n = 0.5, 1), Figs. 2d to 2e. In the case of graphyne, fluorination and chlorination of graphyne shows almost a similar feature and mono absorption peak in fluorinated and also chlorinated graphyne confirm that. The obvious difference between

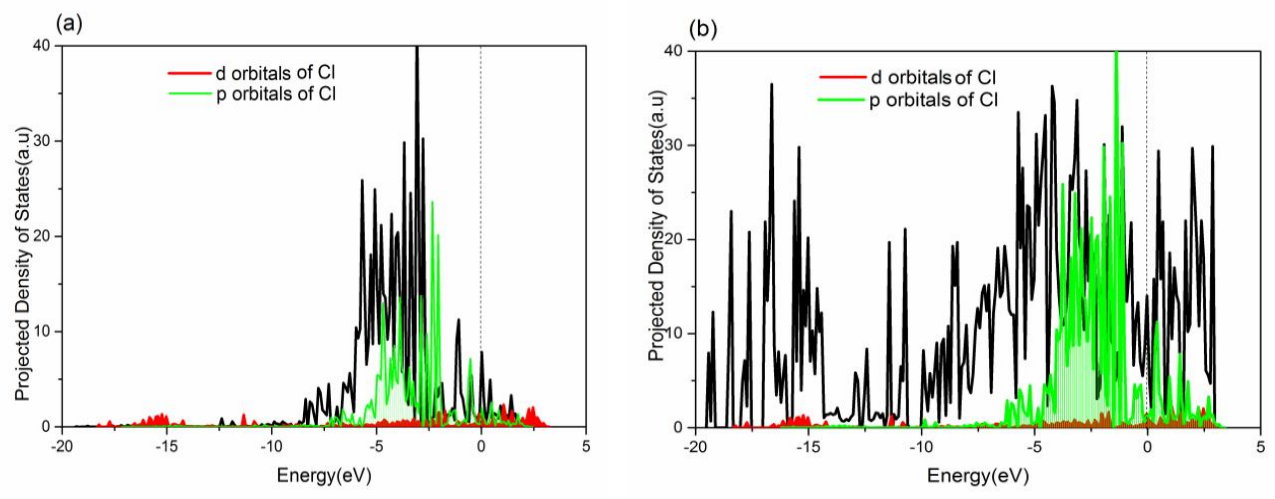

Fig. 4. Projected density of states for (a) pGD-Cl (n = 0.5) (b) pGD-Cl (n = 1).

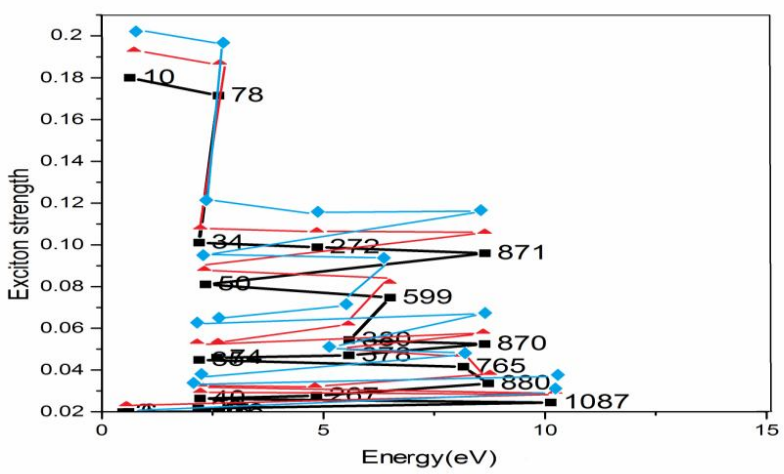

Fig. 5. Energy as a function of exciton strength in pGY [black], pGY-F (n = 0.5) [red] and pGY-F (n = 1) [blue] at the same BSE states.

absorption intensity of fluorinated graphyne (450) and chlorinated graphyne (50) is a remarkable feature of this structure observed in case of graphdiyne but in an opposite way for fluorinated graphdiyne (~10) and chlorinated graphdiyne (~250).

Projected density of states for pGD-Cl (n = 0.5, 1) are illustrated in Fig. 4. The local density of states for p orbitals of chlorine atoms indicates that electrons occupying this level of energy have not any effective contribution in Fermi level of energy. Figure 4 also shows that in n = 0.5, Fermi level of energy is more occupied. Halogenated graphdiyne with n = 0.5 has a remarkable occupied energy state (2.5 eV) around the Fermi level but this occupied state in n = 1 shifts towards the Fermi level (1.5 eV). By comparing total projected density of states in valence shell of n = 1 with n = 0.5 which have the same number of carbon atoms (Figs. 4a and b), one can see that the injection of electrons from chlorine atoms to sheet obviously increases the occupation

of valence bands of carbon atoms.

The strength of electron-hole bonding and effect of halogen concentration on this feature have been studied for clarifying the high excitonic effect on absorption spectra here. The exciton strength for pure graphyne and fluorinated graphyne for n = 0.5 and 1 are compared in Fig. 5. In the same BS states, the excitons are stronger when n = 1. Figure 5 also indicates that in BS states with 2.5 eV, electron-hole bonds are more stable than other energy levels.

CONCLUSIONS

The electronic and structural properties of a single-layer graphdiyne (graphyne) sheet have been studied. Adsorption of halogens can effectively modulate the structural and electrical properties of these structures. The halogenated pGD (pGY) are semiconductor with different band gap values. The Tamm-Dancoff approximation for the BSE Hamiltonian was employed and optical spectra for pGD (pGY) and halogenated pGD (pGY) were obtained from solving BSE equation. The imaginary part of the macroscopic dielectric function shows that pGD (pGY) exhibits exciton effect and high bounded excitons.The calculated cohesive energy for halogenated pGD (pGY) indicates that their stability is in a same range as pGD (pGY). The high stability in all cases is originated from carbon-carbon triple bonds. According to mechanical stability and high bonding energy excitons in these structures one can avocets that halogenated pGD and pGY are good candidates for optoelectronics devices.

ACKNOWLEDGMENTS

F. H deeply appreciates YAMBO committee for very useful discussions. This research was enabled in part by support provided by WestGrid (www.westgrid.ca) and Compute Canada Calcul Canada (www.computecanada.ca).

REFERENCES

[1] Karlicky, F.; Datta, K. K. R.; Otyepka, M.; Zboril, R., Halogenated graphenes: rapidly growing family of graphene derivatives. *ACS Nano*, **2013**, *7*, 6434-6464, DOI: 10.1021/nn4024027.

[2] Wang, Y.; Lee, W. C.; Manga, K. K.; Ang, P. K.; Lu, J.; Liu, Y. P.; Lim, C. T.; Loh, K. P., Fluorinated graphene for promoting neuro-induction of stem cells. *Adv. Mater.*, **2012**, *24*, 4285-4290, DOI: 10.1002/ adma.201200846.

[3] Gong, P.; Yang, Z.; Hong, W.; Wang, Z.; Hou, K.; Wang, J.; Yang, S., To lose is to gain: Effective synthesis of water-soluble graphene fluoroxide quantum dots by sacrificing certain fluorine atoms from exfoliated fluorinated graphene. *Carbon*, **2015**, *83*, 152-161, DOI: 10.1016/j.carbon.2014.11.027.

[4] Zhu, S.; Li, T., Wrinkling instability of graphene on substrate-supported nanoparticles. *J. Appl. Mech.*, **2014**, *81*, 061008, DOI: 10.1115/1.4026638.

[5] Marsden, J. A.; Haley, M. M., Carbon networks based on dehydrobenzoannulenes. 5. Extension of two-dimensional conjugation in graphdiyne nanoarchitectures. *J. Org. Chem.*, **2005**, *70*, 1-213-10226, DOI: 10.1021/jo050926v.

[6] Peng, Q.; Dearden, A. K.; Crean, J.; Han, L.; Liu, S.; Wen, X.; De, S., New materials graphyne, graphdiyne, graphone, and graphane: review of properties, synthesis,and application in nanotechnology. *Nanotechnol. Sci. Appl.*, **2014**, *7*, 1-29, DOI: 10.2147/NSA.S40324.

[7] Qian, X.; Liu, H.; Huang, C.; Chen, S.; Zhang, L.; Li, Y.; Wang, J.; Li, Y., Self-catalyzed growth of lare-area nanofilms of two-dimensional carbon. *Sci. Rep.*, **2015**, *5*, 7756, DOI: 10.1038/srep07756.

[8] Jalili, S.; Houshmand, F.; Schofield, J., Study of carrier mobility of tubular and planar graphdiyne. *Appl. Phys. A*, **2015**, *119*, 571-579.

[9] Luo, G.; Qian, X.; Liu, H.; Qin, R.; Zhou, J.; Li, L.; Gao, Z.; Wang, E.; Mei, W. N.; Lu, J.; Li, Y.; Nagase, S., Quasiparticle energies and excitonic effects of the two-dimentional carbon allotrope graphdiyne: Theory and experiment. *Phys. Rev. B*, **2011**, *84*, 075439, DOI: 10.1103/PhysRevB.84.075439.

[10] Luo, G.; Zheng, Q.; Mei, W. N.; Lu, J.; Nagase, S., Structural, electronic and optical properties of bulk

graphdiyne. *J. Phys. Chem. C*, **2013**, *117*, 13072-13079, DOI: 10.1021/jp402218k.

[11] Wang, Chengliang, *et al*. Semiconducting π-conjugated systems in field-effect transistors: a material odyssey of organic electronics. *Chem. Rev.*, **2012**, *112*, 2208-2267, DOI: 10.1021/cr100380z.

[12] Matthew, J., Amanda E. *et al*. Porphyrins as molecular electronic components of functional devices. *Coord. Chem. Rev.*, **2010**, *254*, 2297-2310. DOI: 10.1016/j.ccr.2010.05.014.

[13] Kim, F. S.; Guoqiang R.; Samson, A. J., One-dimensional nanostructures of π-conjugated molecular systems: assembly, properties, and applications from photovoltaics, sensors, and nanophotonics to nanoelectronics. *Chem. Mater.*, **2010**, *23*, 682-732.

[14] Hunter, C. A.; Sanders, J. K. M., The nature of Pi-Pi interactions. *J. Am. Chem. Soc.*, **1990**, *112*, 5525-5534, DOI: 10.1021/ja00170a016.

[15] Giannozzi, P.; Baroni, S.; Bonini, N.; Calandra, M.; Car, R.; Cavazzoni, C.; Ceresoli, D.; Chiarotti, G. L.; Cococcioni, M.; Dabo, I.; Dal Corso, A.; de Gironcoli, S.; Fabris, S.; Fratesi, G.; Gebauer, R.; Gerstmann, U.; Gougoussis, C.; Kokalj, A.; Lazzeri, M.; Martin-Samos, L.; Marzari, N.; Mauri, F.; Mazzarello, R.; Paolini, S.; Pasquarello, A.; Paulatto, L.; Sbraccia, C.; Scandolo, S.; Sclauzero, G.; Seitsonen, A. P.; Smogunov, A.; Umari, P.; Wentzcovitch, R. M., QUANTUM ESPRESSO: A modular and open-source software project for quantum simulations of materials. *J. Phys. Condens. Mat.*, **2009**, *21*, 395502, DOI: 10.1088/0953-8984/21/39/395502.

[16] Hartwigsen, C.; Sephen, G.; Jürg, H., Relativistic separable dual-space Gaussian pseudopotentials from H to Rn. *Phys. Rev. B*, **1998**, *58*, 3641, DOI: arXiv:cond-mat/9803286v1.

[17] Marini, A.; Hogan, C.; Grüning, M.; Varsano, D., Yambo: An *ab initio* tool for excited state calculations. *Comput. Phys. Commun.*, **2009**, *180*, 1392-1403, DOI: 10.1016/j.cpc.2009.02.003.

[18] Soler, J. M.; Artacho, E.; Gale, J. D.; Garcia, A.; Junquera, J.; Ordejon, P.; Sanchez-Portal, D., The SIESTA method for *ab initio* order-N materials simulation., **2002**, *14*, 2745, DOI: 10.1088/0953-8984/14/11/302.

[19] Henkelman, G.; Uberuaga, B. P.; Jonsson, H., A climbing image nudged elastic band method for finding saddle points and minimum energy paths. *J. Chem. Phys.*, **2000**, *113*, 9901, DOI: 10.1063/1.1329672.

[20] Chantharasupawong, P.; Philip, R.; Narayanan, N. T.; Sudeep, P. M.; Mathkar, A.; Ajayan, P. M.; Thomas, J., Optical power limiting in fluorinated graphene oxide: An insight into the nonlinear optical properties. *J. Phys. Chem. C*, **2012**, *116*, 25955-25961, DOI: 10.1021/jp3096693.

[21] Koo, J.; Huang, B.; Lee, H.; Kim, G.; Nam, J.; Kwon, Y.; Lee, H., Tailoring the electronic band gap of graphyne. *J. Phys. Chem. C*, **2014**, *118*, 2463-2468, DOI: 10.1021/jp4087464.

[22] Osuna, S.; Torrent-Sucarrat, M.; Sola, M.; Geerlings, P.; Ewels, C. P.; Vam Lier, G., Reaction mechanisms for graphene and carbon nanotube fluorination. *J. Phys. Chem. C*, **2010**, *114*, 3340-3345, DOI: 10.1021/jp908887n.

[23] Boukhvalov, D. W.; Katsnelson, M. I., A new route towards uniformly functionalized single-layer graphene. *J. Phys. D Appl. Phys.*, **2011**, *43*, 175302, DOI: 10.1088/0022-3727/43/17/175302.

[24] Caravaca, M. A.; Mino, J. C.; Perez, V. J.; Casali, R. A.; Ponce, C. A., *Ab initio* study of the elastic properties of single and polycrystal TiO_2, ZrO_2 and HfO_2 in the cotunnite structure. *J. Phys. Condens. Mat.*, **2009**, *21*, 015501, DOI: 10.1088/0953-8984/21/1/015501.

[25] Haines, J.; Leger, J. M.; Bocquillon, G., Synthesis and design of superhard materials. *Annu. Rev. Mater. Res.*, **2001**, *31*, 1-23, DOI: 10.1146/annurev.matsci.31.1.1.

[26] Mouhat, F.; Coudert, F. X.; Necessary and sufficient elastic stability conditions in various crystal systems. *Phys. Rev. B*, **2014**, *90*, 224104, DOI: 10.1103/PhysRevB.90.224104.

[27] Ravindran, P.; Fast, L.; Korzhavyi, P. A.; Johansson, B.; Wills, J.; Eriksson, O., Density functional theory for calculation of elastic properties of orthorhombic crystals: Application to $TiSi_2$. *J. Appl. Phys.*, **1998**, *84*, 4891, DOI: 10.1063/1.368733.

[28] Pugh, S. F., Relations between the elastic moduli and the plastic properties of polycrystalline pure metals. *Philos. Mag.*, **1954**, *45*, 823-843, DOI: 10.1080/14786440808520496.

[29] Yu, R.; Zhu, J.; Ye, H. Q., Calculations of single-crystal elastic constants made simple. *Comput. Phys. Commun.*, **2010**, *181*, 671-675, DOI: 10.1016/j.cpc.2009.11.017.